Low-Cost Fabrication and Surface Engineering of Insulating KBr Crystals: An AFM Study on the Effects of Thermal Annealing

Asieh sadat Kazemi*, Maryam Hashemi, Mohamad Mohamadnezhad

Surface Physics Lab, Department of Physics, Iran University of Science and Technology
**Corresponding Author: asiehsadat_kazemi@iust.ac.ir*

Abstract

Potassium bromide (KBr) crystal structure attracts attention due to its various applications in electronic and optical devices as well as its potential in inducing local electrostatic fields. Fabricating this crystal via the conventional Czochralski method or more novel epitaxial methods is very costly. Here, with the focus on surface properties, a simple low-cost technique is employed based on the usage of KBr powder, pellet making, and pressure appliance for the fabrication of pellet crystals. These pellets have been annealed at various temperatures and studied via atomic force microscopy; morphologically and structurally. Our results demonstrate that increasing the temperature before the KBr melting point significantly reduces different roughness parameters, the height of the atomic steps, and the distance between them. At 500 °C, the atomic steps are more regular than at other temperatures, surface flatness and crystallinity are enhanced, approaching the quality of commercial single crystals. These modifications improve the quality of the crystals significantly, for various applications. Force spectroscopic measurements across atomic step edges of KBr, demonstrates higher forces with respect to flat regions. These engineered steps could serve as nanoscale templates for directing the self-assembly of molecules or for creating spatially varying electrostatic potentials in 2D material heterostructures.

Keywords: KBr crystal, AFM, Atomic steps, Roughness, Force spectroscopy

1- Introduction

KBr has a clear and uniform FCC crystal, it is highly transparent in the mid-infrared (IR) region and non absorbing for most IR wavelenghts, also has high permeability and wide bandwidth [1], commonly used in IR fourier transform spectroscopy (FTIR) and beam splitters in

[DOI: 10.22068/ijmse.3566]

spectrophotometers due to its low phonon absorption and in scintillators [2, 3]. KBr is also colorless and due to its ionic nature, is soluble in water, and has a melting point of 734 °C. KBr substrates are soft and moist, and have good resistance to mechanical shocks [4]. Since they cleave easily along (100) planes, they are used for thin film growth [5], in the production of soft electronic components as an electrical insulator, and as a supprot for molecular adsorption stuides in UHV systems [6]. Terrace modifications of KBr as an ionic substrate at an atomic level has been used as a source to generate electrostatic potentials on 2D materials [7]. KBr pellets are recently used to assess the photodimerazation (i.e. the photochemical reaction) of acid compounds [8]. Furthermore, KBr is used as a light transducer in the range of 10-200 nm ultraviolet and soft X-ray components [9]. KBr thin films are feasible alternatives for ultraviolet (UV) and soft X-ray photocathode devices due to their high quantum efficiency and good stability in the extreme ultraviolet to vacuum ultraviolet regions [10]. They can also be used as a proatective layer in visible-sensitive photon detectors [11]. Owing to lower photoconversion efficiency of KBr photocathode in the far ultraviolet (FUV) wavelength region, signal quality may be improved by rejecting the sources of radiation and background near UV wavelengths [12]. The crystal surface in many oxides and alkali halides such as KBr, is different to their corresponding bulk due to the presence of dangling bonds and partly by surface irregularities such as dislocations, vacancies and defects in the periodicity of the crystal. These surface features and broken periodicity at the termination planes can evolve dynamically under environmental influences like vapor adsorption; leading to distinct surface energies and structural rearrangements [13, 14] which highlights the importance of dedicated surface studies to understand real material behavior beyond ideal bulk lattice models.

A monocrystalline solid is a material in which the crystal lattice of the entire sample, from the mass to the edges of the piece, is continuous and unbroken. The absence of defects gives single crystals unique mechanical, optical, and electrical properties with respect to polycrystals [15]. Specific methods for producing single crystals include the Czochralski process, the floating zone process, and the Bridgeman method [16,17], where some like the Chekralski's furnace cost between $400,000 and $1 million at least. The main techniques of KBr crystal growth can be divided into four categories: molten, solid, vapor, and soluble. Other crystallization methods vary depending on the material's physical properties, such as hydrothermal synthesis, sublimation, simple solvent-based crystallization [6] or epitaxy [18]. The laying method is used to place skinny

[DOI: 10.22068/ijmse.3566]

layers (micro or nanometer) of similar or different materials on the surface of a crystal. This method has been influential in producing polar plates (111) of potassium bromide, which is electrostatically unstable under normal conditions [19]. However, vacuum-based assembly methods are very expensive and increase the cost of crystal production.

With regards of the importance of surface studies and the critical conditions of surface quality for the mentioned applications, and due to the existence of the current expensive methods, we report a simple, low-cost approach to achieve high quality flat KBr surfaces followed by thorough characterizations to find the optimal conditions. In the inexpensive method, transparent pressurized pellets were heated at different temperatures in the furnace and examined with an optical microscope. Water evaporation mechanism at different annealing temperatures in KBr pellets were explored by FTIR while the overal crystal structure of the pellets was investigated by X-ray diffraction (XRD). The surface morpholgy, step edges. roughness and adhesive force of these crystals were characterized by atomic force microscopy (AFM) in contact mode and compared to standard KBr substrate in terms of surface flatness, number and distance of the atomic steps at various annealing temperatures.

2- Materials and Methods

Spectroscopic-grade quality KBr powder (Merck) with a particle size of 100–200 mesh (~100 μm) [18], was first grinded in a unique, pre-cleaned opal mortar to give a uniform texture. The softened powder was placed evenly inside the 1 cm diameter pellet holder. The holder containing the uniform powder was placed in a press unit, and the pellets were fabricated using a laboratory hydraulic pellet press with maximum capacity of 15 tons. The powder was pressed in a 1 cm diameter die, applying approximately 8 tons-force. With the similar method, several pellets were fabricated for reproducibilty purposes and to use for annealing at various temperatures. Next, the pellets were placed in clean ceramic boats and into the furnace. The furnace was heated up in 50 °C steps to reach the desired temperatures at 350 °C, 400 °C, 450 °C, 500°C, 550°C and 600 °C, and kept for an hour. Then the furnace temperature was reduced stepwise to room temperature (RT) to prevent heat shock on the pellets. All samples were kept in a vacuum desiccator. For comparison study, a KBr (100) crystal was purchased from *Agar Scientific* with the trade ID AGG3900, cleaved at a right angle with a sharp blade. FTIR spectroscopy (Perkin Elmer 100) was performed on all pellets before the annealing process. Crystallography was achieved on the

[DOI: 10.22068/ijmse.3566]

samples with X-ray diffration (XRD) system (Bruker-Advanced) and further analyses on the crystal planes and orientations were investigated with *XPert* software. FTIR and XRD results and discussions are presented in Supporting Information (SI). Topography imaging and force spectroscopy were accomplished with an atomic force microscope (Advanced-Ara Pajuhesh) at RT with humidity of 30 % where KBr surface stays safe. Contact mode with low force was used with HQ:CSC17/AlBS cantilever purchased from MikroMasch, with force constant of 0.18 N/m and resonance frequency of 13 kHz. The material of the cantilver was n-type Si. These AFM cantilevers with low force constants offer high sensitivity in contact mode, high consistency of tip radius, cantilever reflectivity and the quality factor. The set point was kept at 0.65 of reference voltage and the and the can rate was 1 line/s.

3. Results and discussion

3.1. Atomic steps

The formation of atomic steps of KBr at temperatures 350 ℃, 400℃, 450℃, 500℃, 550℃, and 600 ℃ was investigated using AFM. These measurements on the surface of the KBr unveiled terraces of widths between 1.40 μm and 6 μm. Figure 1 shows 2D and 3D AFM images of KBr surfaces in contact mode. On the surface of KBr at 350 °C, there appears no specific atomic steps in the imaging window, but they may be much farther away. It is evident that the distance between the atomic steps decreases with the increase in temperature, thus, the atomic steps become closer. In addition, the height of the steps decreases with the increase in temperature. Borderline-like lines on the surface of the images may be due to stresses created in the pellet-making process and appear to be visible in all images, regardless of the annealing temperature. At 500 °C, the atomic steps are more regular and sharper than at other temperatures. As the temperature increases to 550 °C and 600 °C, the atomic steps start to merge, lose regularity and become rounded, transitioning towards lower energy steps. As the pellets approach their melting point, their crystal structure deteriorated, in agreement with the evolution of XRD spectra in SI, where the intensity of the peaks was the highest at 450 °C and 500 °C. Figure 2 (b) shows the variation of distance between the atomic steps in annealed KBr pellets with temperature. With the increase in temperature, the distance between the atomic steps decreased. These data were extracted by processing images with SPIP software.

[DOI: 10.22068/ijmse.3566]

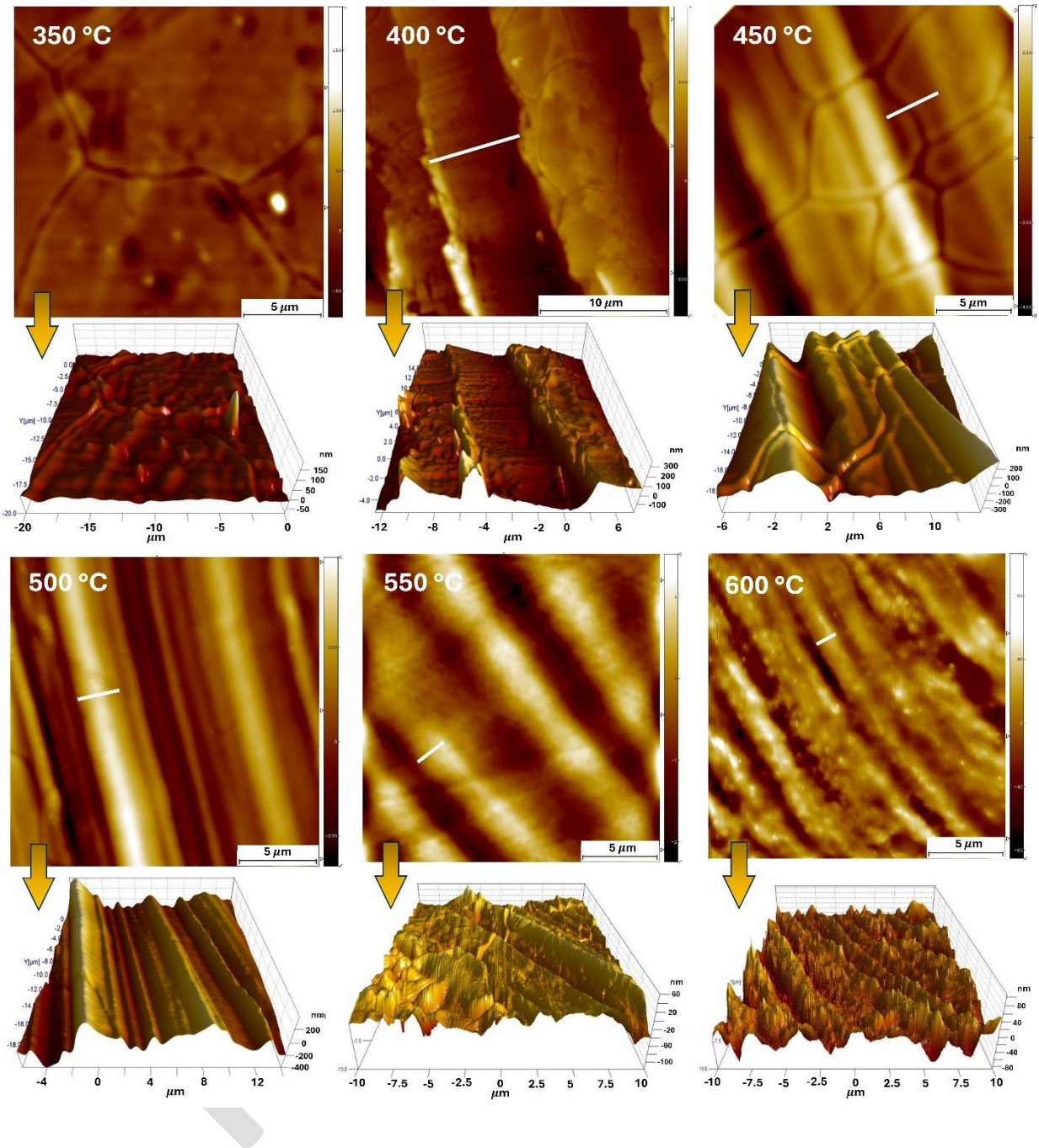

Figure 1. 2D and the corresponding 3D AFM topographic images of the surface of KBr pellets in contact mode at different annealing temperatures; all with dimensions of 20μm×20 μm.

The observed rounding and straightening of the step edges during annealing indicate a transition from higher-energy, high-Miller-index facets toward lower-energy, low-Miller-index facets, consistent with thermodynamically favored surface restructuring in agreement with [20, 21]. Figure 2 (c) schematically shows the evolution of high index steps into low index steps with the

[DOI: 10.22068/ijmse.3566]

increase in annealing temperature at a cubic crystal step edge. Although the atomic sized transitions beyond 500 °C need to be featurd with high resolution microscopes like tuning fork non-contact AFM, but evidences of step boundary features can be in seen on the surface of 500 °C sample in Figure 2 (a) where a boat shaped is enlarged. This shape can constitute many high index steps if atomically resolved. 2D and 3D AFM images of the as-purchased crystalline KBr as a reference for this study in Figures 2 (d,e) show ultra-regular atomic steps with very short distances. The steps in KBr pellets at 500 °C are closests to this sample.

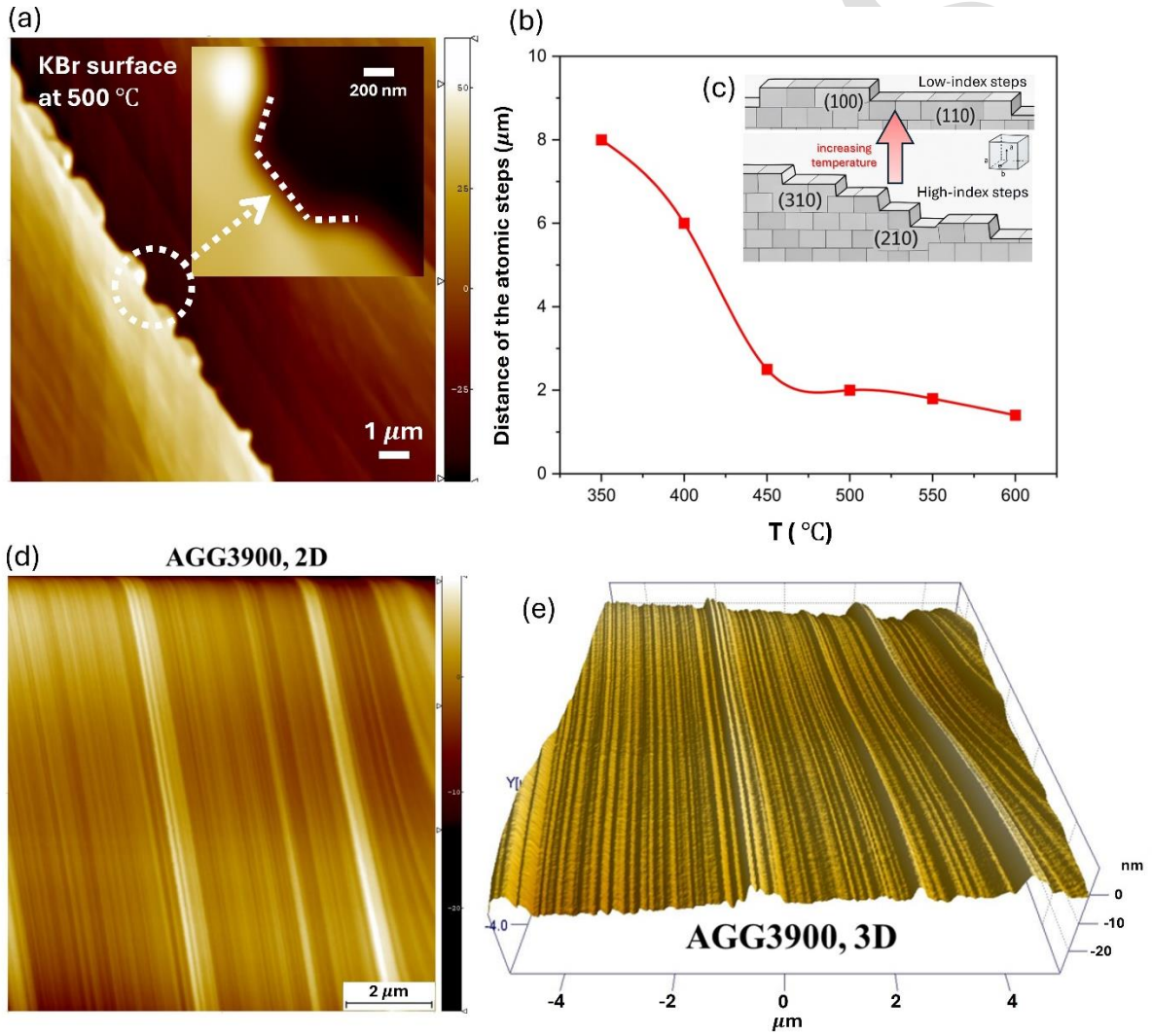

Figure 2. (a) 2D AFM image of a step edge with boat shape boundary, (b) The average distances of the atomic steps in annealed KBr samples at different temperatures, (c) Schematics of step transitions with the increase in temperature, (d,e) 2D and 3D images of *AGAR Scientific* KBr crystal with trade ID AGG3900.

[DOI: 10.22068/ijmse.3566]

3.2. Roughness variation with annealing temperature

Accurate surface roughness study on KBr at different annealing temperatures required equal sized imaging windows without the presence of the atomic steps or stress boundaries. Therefore, 2μm×2μm windows were isolated from 2D images in Figure 1 in a region between a pair of atomic steps depicted in Figure 3(a). The roughness parameters of these images were processed with SPIP software and summarized in Figure 3(b). Roughness parameters of reference sample was also extracted for comparison. Sa, being the most common rougness parameter reported in the literature, as the average roughness, or the average of the deviations from the mean plane varied with annealing temperature as shown in Figure 3(c). Sq is the RMS roughness and also commonly used which is the standard deviation of the height distribution. Sz is the difference between Sp and Sv, while Sp shows maximum peak height and Sv shows maximum valley depth. The surface roughnesses, or Sa, decreased markedly with increase in annealing temperature up to 500°C. Beyond that, Sa increased rapidly to values higher than 5 nm. Again, from previous analyses, it is known that beyond this point, crystallinity of the surface deteriorates. Another quantity extracted from the surface roughness, Sq, has similar variation as Sa. The other two standard parameters, Sp and Sv, indicated small variations (below 10 nm) in refrence KBr and those annealed at 400 °C, 450 °C and 500 °C. However, at 350 °C, 550 °C and 600 °C, these parameters rise to much higher values up to 50 nm. Sz, bieng calculated from Sp and Sv, showed similar trend. This means highest peak height and deepest valley depth in less crystalline samples are higher and this agrees with XRD results.

In short, the initial reduction in surface roughnesses up to 500 °C can be attributed to enhanced surface diffusion and increased atomic mobility, which promote the relaxation of surface irregularities, step edges and the elimination of defects in agreement with [22]. At higher temperatures, however, all roughness values increased rapidly, likely due to surface instability, defect formation, and partial degradation of surface crystallinity as the material approached thermally activated disordering or pre-melting phenomena as commonly observed for alkali halide surfaces such as KBr.

[DOI: 10.22068/ijmse.3566]

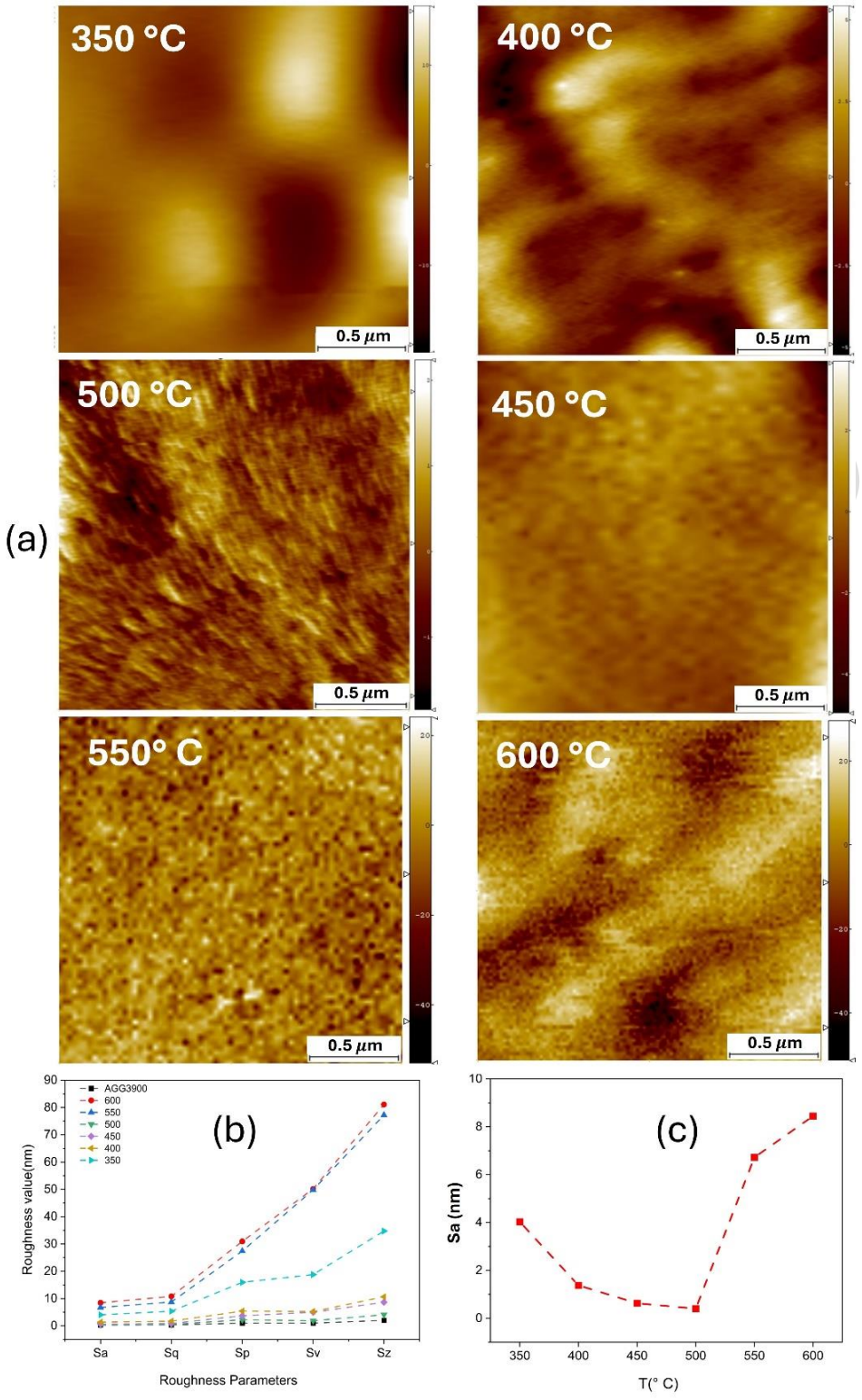

Figure 3. (a) 2D topographic images of the surface of KBr pellets at different annealing temperatures, (b) Variation of roughness parameters extracted from the 2D images in part (a), (c) Sa variation with annealing temperature.

[DOI: 10.22068/ijmse.3566]

3.3. Force spectroscopy across atomic steps

According to the AFM roughness and XRD results, annealed KBr samples arount 500 °C demonstrated higher degree of crystallinity. Some of the samples were selected for force spectroscopy. This process was done point by point on the surface by swithing off the feedback loop and implementing a certain value of indentation onto the substrate, enabling pull-off force (as the maximum attractive force during tip retraction in each force–distance curve) detection. Figure 4 shows 2D images of atomic steps of KBr pellets annealed at 450 °C, 500 °C, 550 °C and the reference purchased KBr. Force spectroscopy was performed with only a few nanometers indentation, well within the elastic deformation regime and non-destructive for the KBr crystal. The force variation data across these steps in nN demonstrated higher forces at the boundary of the steps while flatter regions had lower adhesive forces. The increased adhesion observed at the step edges can be attributed to the higher local surface energy at these sites. Step edges and defect sites are more likely to adsorb ambient water molecules, which enhances capillary forces. In addition, the intrinsic ionic polarization at the step may increase local electrostatic interactions between the tip and surface, further contributing to the elevated adhesive force [23]. This property of atomic steps can be exploited in electrostatic potential tuning on the bare KBr or KBr covered with 2D materials where screening effects are still minor as predicted theoretically and demonstrated by electric force microscopy and scanning tunneling microscopy/spectroscopy in [24, 25].

[DOI: 10.22068/ijmse.3566]

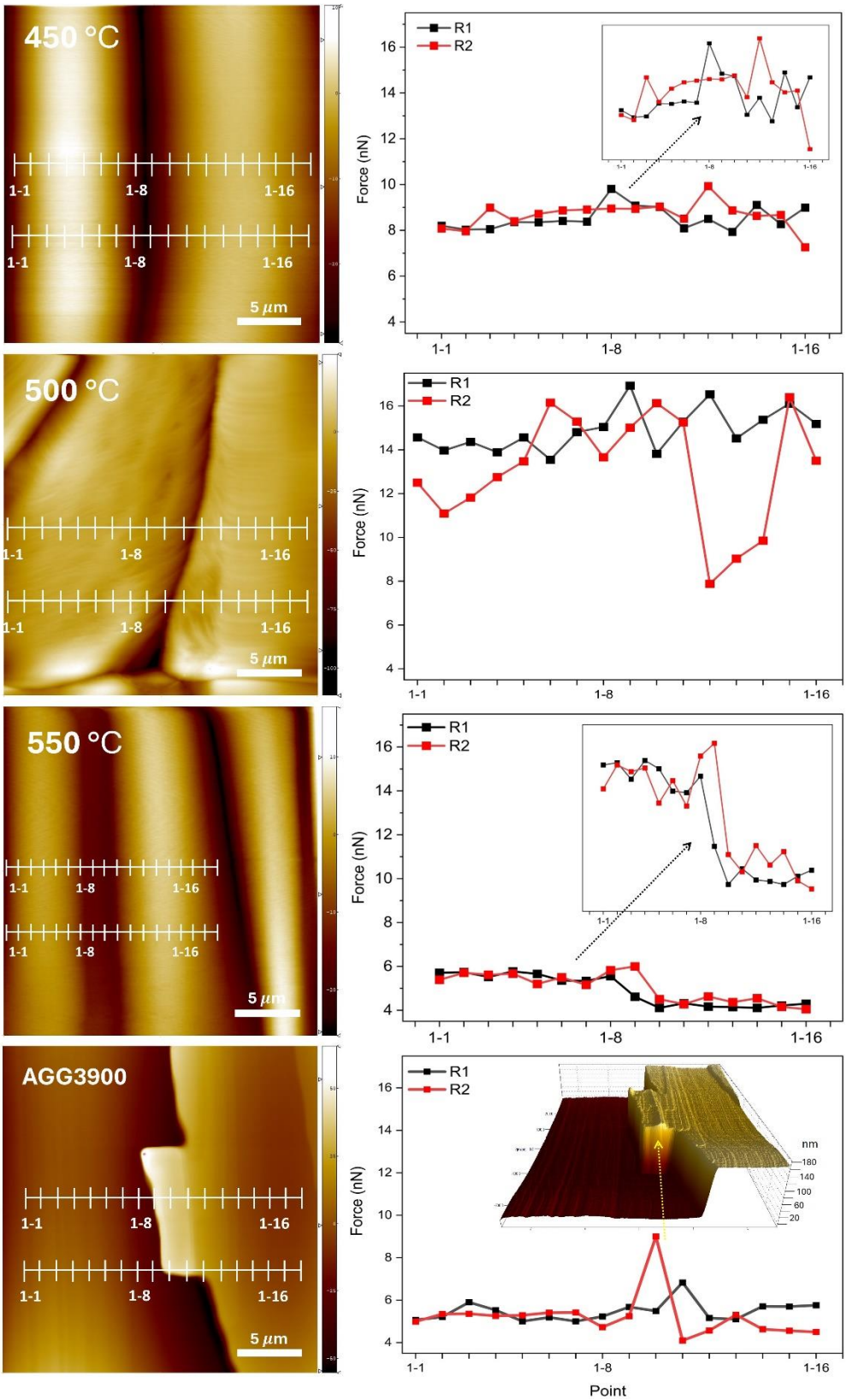

Figure 4. 2D AFM topographic images of KBr samples at 450 °C, 500 °C, 550 °C and the reference KBr sample along with pull-off force variations across relevant atomic steps.

[DOI: 10.22068/ijmse.3566]

3.4. FTIR and XRD analyses

The evolution of water with annealing temperature in KBr pellets was examined via FTIR spectroscopy in SI and Figure S1. The results were in agreement with [2,26,27]. XRD data were collected from pellets using monochromated CuKα (λ=1.54060 Å) radiation with 2θ from 5° to 85°. XRD spectra of the annealed pellets are depicted in Figure S2 confirming an FCC crytal structure and agrees with the literature [28]. XRD patterns of KBr pellets exhibit the most intense peak at the (200) crystallographic plane; this peak is from the peak family of (100) and is essential in potassium bromide crystals, followed by other peaks at (111), (220), and (420) planes, respectively. For better clarity, significant peaks are zoomed in Figure 1. The zoomed in image of (111) peak at 350 °C and 400 °C shows low intensity. At 450 °C and 500 °C, the intensity of this peak increases. With further increase in annealing temperature to 550 °C and 600 °C, the intensity of this peak decreaces to its lowest value in agreement with [29, 30].

4- Conclusions

Unexpensive and simple was used to produce KBr crystal structures and tune crystal properties based on pressurized powder and annealing process. KBr has many application across different fields and easier fabrication of this material with tuned crystallinity is desired. Structural and morphological study along with intensive AFM imaging, roughness measurement and force spectroscopy was performed on KBr samples annealed at 350 °C to 600 °C just below its melting temperature and on a reference KBr substrate purchased for comparison. The results demonstrated that the optimal annealing temperature was 500 °C, where higher crystallinity occurred on the surface, best agreement with the reference sample was observed, average roughness Sa was reduced to 0.4 nm and step spacing reduced to 2 μm. Force spectroscopy measurements demonstrated larger adhesive force on the atomic steps with respect to flat regions. We propose that these engineered steps could serve as nanoscale templates for directing the self-assembly of molecules or for creating spatially varying electrostatic potentials in 2D material heterostructures, which could be probed by Kelvin Probe Force Microscopy (KPFM).

[DOI: 10.22068/ijmse.3566]

5- References

[1] Singh, S. P., et al., Optical and luminescence properties of alkali halide crystals, Journal of Luminescence, 2008, 128, 1379–1384.

[2] Chalmers, J., Infrared spectroscopy, Encyclopedia of Analytical Science (Second Edition), Elsevier, 2005, 402-415.

[3] Lin, L. Y. et al., Study of scintillation stability in KBr, YAG:Ce, CaF2:Eu and CsI:Tl irradiated by various-energy protons, International Beam Instrumentation Conference, 2014, IBIC.

[4] Villars, P., KBr Crystal Structure, Pauling File Multinaries Edition in: Inorganic Solid Phases, Springer Materials, Springer, 2023, Heidelberg (ed.) SpringerMaterials.

[5] Xu, T., Cai, Q., Duan, W., Wang, K., Jia, B., Luo, H., & Liu, D., Effect of Substrate Temperature on the Structural, Morphological, and Infrared Optical Properties of KBr Thin Films. Materials, 2025, 18(15), 3644.

[6] Glatzel, T., Zimmerli, L., Kawai, S., Meyer, E., Fendt, L. A. & Diederich, F., Oriented growth of porphyrin-based molecular wires on ionic crystals analyzed by NC-AFM, Beilstein J. Nanotechnol., 2011, 2, 34–39.

[7] Jones, G. J., Kazemi, A., Crampin, S., Phillips, M., Ilie, A., Surface Potential Variations in Graphene Induced by Nanostructured Crystalline Ionic Substrates, Applied Physics Express, 2012, 5 (4), 045103.

[8] Ulambayar, B., Batchuluun, K., Bariashir, C., Uranbileg, N., Stammler, F. J., Davaasambuu, J., & Schrader, T. E., Using potassium bromide pellets and optical spectroscopy to assess the photodimerization of two trans-(trifluoromethyl)-cinnamic acid compounds. CrystEngComm, 2024, 26, 4470–4477.

[9] Rai, R., Triloki, Singh, B. K., Photoemission and morphological studies of KBr thin-film photocathode for astrophysics application, Proceedings of the DAE-BRNS Symp. on Nucl. Phys. 2016, 61.

[10] Oswald H.W. Siegmund, E. Everman, J.V. Vallerga et al., Ultraviolet quantum detection efficiency of potassium bromide as an opaque photocathode applied to microchannel plates, Appl. Opt. 1987, 26, 3607.

[DOI: 10.22068/ijmse.3566]

[11] Breskin, A., Buzulutskov, A., Chechik, R. et al., Evidence for thin film protection of visible photocathodes, Appl. Phys. Lett., 1996, 69, 1008.

[12] Oswald H.W. Siegmund, D.E. Everman, J.V. Vallerga et al., Soft x-ray and extreme ultraviolet quantum detection efficiency of potassium bromide photocathode layers on microchannel plates, Appl. Opt., 1988, 27, 1568.

[13] Alherz, A., & Alayyoub, B. A., Evaluation of Surface and Bulk Properties of Alkali Halides: A First-Principles Study on (100) and (110) Facets, ACS Omega, 2025, 10(44), 52794–52803.

[14] Pokorny, P., Novotny, M., Dekhtyar, Y., Lushchik, A., Hruska, P., Fara, J., Fitl, P., Musil, J., Jaaniso, R., Lancok, J., Surface processes on KBr single crystals examined by thermostimulated exo-electron emission and desorption, Optical Materials, 2021, 114, 110898.

[15] Milisavljevic, I., Wu, Y., Current status of solid-state single crystal growth, BMC Mat, 2020, 2**,** 2.

[16] Müller, G., Friedrich, J., Crystal growth, bulk: methods. In: Bassani G, Liedl G, Wyder P, editors. Encyclopedia of condensed matter physics. Oxford: Elsevier Ltd; 2005, 262–74.

[17] Suan Jen Hsueh Pao, K., Growth Process of Large Section Crystal of Potassium Bromide, Journal of the Chinese Ceramic Society, 2015, 43(1), 60-64.

[18] Kato, S., Takeyama, Y., Maruyama, S., and Matsumoto, Y., Nonfaceted Growth of (111)-Oriented Epitaxial Alkali-Halide Crystals via an Ionic Liquid Flux in a Vacuum, Crystal Growth & Design, 2010, 10(8).

[19] Yamauchi, M., Maruyama, S., Ohashi, N., Toyabe, K. and Matsumoto, Y., Epitaxial growth of atomically flat KBr(111) films via a thin ionic liquid in a vacuum, Cryst. Eng. Comm, 2016, 18, 3399.

[20] Bonzel, H. P., Equilibrium crystal shapes and surface faceting, Progress in Surface Science, 2003, 67(1–3), 45–70.

[21] Erb**,** D. J., Perlich, J., Roth, S. V. Ralf, Schlage, K., Real-Time Observation of Temperature-Induced Surface Nanofaceting in M-Plane α-Al_2O_3, ACS Appl. Mater. Interfaces, 2022, 14, 27, 31373–31384.

[DOI: 10.22068/ijmse.3566]

[22] Parida, S., Lacasa, J. S., & Eren, B. Water vapor and alcohol vapor induced healing of the nanostructured KBr surface, The Journal of Physical Chemistry C, 2022, 126(31), 13433–13440.

[23] Snyder, R. G., & Scoles, G. Surface and step-edge effects on adhesion forces measured by AFM, Langmuir, 1991, 7, 2321–2327.

[24] Wu, Y., Computational Studies of Graphene on Nanostructured Ionic Substrates, Ph.D. Thesis, University of Bath, 2016.

[25] Kazemi, A. S., Engineering the wavefunction in graphene systems, Ph.D. Thesis, University of Bath, 2015.

[26] Khajelakzay,_M., Shoja Razavi,_R., Barekat,_M., Synthesis and Characterization of Yttria Nanopowders by Precipitation Method, Transactions of the Indian Ceramic Society, 2015, 74(4), 208-212.

[27] Gordon, S. H., Mohamed, A., Harry-O'Kuru, R. E., Imam, S. H., A Chemometric Method for Correcting Fourier Transform Infrared Spectra of Biomaterials for Interference from Water in KBr Discs. Applied Spectroscopy, 2010, 64(4), 448-457.

[28] R. Rai, T. Triloki, B.K. Singh, X-ray diffraction line profile analysis of KBr thin films, Appl. Phys. A, 2016, 122, 774.

[29] Liu, Y., Song, H., Zhang, Q., and Chen, D., A Preliminary Study of the Preparation of a KBr-Doped ZnO Nanoparticle and Its Photocatalytic Performance on the Removal of Oil from Oily Sewage, Ind. Eng. Chem. Res., 2012, 51 (13), 4779–4782.

[30] Unga´r, T., Balogh, L., Riba´rik, G., Defect related physical profile based X ray and neutron line profile analysis, Metall. Mater. Trans. A, 2010, 41, 1202.

[DOI: 10.22068/ijmse.3566]